

Active Species Generation in Gas–liquid Discharge Non-thermal Plasma: Operating Conditions, Influencing Factors, and Mechanisms

Keke Ma¹, Lu Zhou^{1,*}, Bai Yu¹, Yiyang Xin¹, Zhi Cao¹, Heping Li², Chengyu Bao², Yuexi Zhou^{1,3}

¹ School of Environment, Tsinghua University, Beijing 100084, P. R. China

² Department of Engineering Physics, Tsinghua University, Beijing 100084, P. R. China

³ Research Center of Environmental Pollution Control Engineering Technology, Chinese Research Academy of Environmental Sciences, Beijing 100012, P.R. China

*E-mail: zhoulu@tsinghua.edu.cn

Received: 7 February 2021 / Accepted: 31 March 2021 / Published: 30 April 2021

In this study, gas–liquid phase non-thermal plasma in a needle-plate reactor was used to evaluate the generation of active species ($\cdot\text{OH}$, H_2O_2 , and O_3). Specifically, the effects of different factors, including initial pH, conductivity, gas flow rate, and solution circulation flow rate, on the generation of these active species were investigated. Tert-butanol (TBA) was chosen as the scavenger of $\cdot\text{OH}$ given that formaldehyde is a specific product of their reaction. The results showed that the generation of $\cdot\text{OH}$ and H_2O_2 occurs at a faster rate in acidic solutions than in alkaline and neutral solutions. High-conductivity solutions hindered the generation of these active species, which were also affected by the electrolyte type. Further, oxygen and liquid circulation flow rates had little effect on $\cdot\text{OH}$ and H_2O_2 generation in aqueous solutions. However, they exerted a greater impact on ozone mass transfer in gas and liquid phases. Furthermore, the simulation of the effects of UV irradiation, H_2O_2 oxidation, and ozone oxidation on the generation of these active species during discharge showed that individually, UV radiation and ozone oxidation had no significant effect on the generation of $\cdot\text{OH}$ and H_2O_2 . However, various combinations of these processes, especially UV/ $\text{O}_3/\text{H}_2\text{O}_2$ and UV/ O_3 , significantly enhanced $\cdot\text{OH}$ production.

Keywords: gas–liquid discharge, non-thermal plasma, active species, hydroxyl radical, mechanism

1. INTRODUCTION

Gas–liquid two-phase non-thermal plasma (NTP) water treatment technology represents a new type of advanced oxidation process. During the discharge process associated with this technology, high-energy electrons are generated owing to the action of a high-intensity electromagnetic field. These electrons collide with water or gas molecules, thereby generating a large number of active free radicals

and oxide species with strong oxidizing properties that promote the degradation of target pollutants until mineralization is realized [1, 2]. This discharge process is often accompanied by various physical processes, such as ultraviolet (UV) light irradiation, high-temperature pyrolysis, and the movement of high-energy electrons as well as shock waves [3-5]. Thus, NTP is a combination of chemical, photochemical, ultrasonic, and electrical processes.

In addition to the generation of high-energy electrons, ionized atoms and molecules, as well as positive and negative ions, NTP processes also involve the generation of active species that play a major role in the degradation of organic contaminants in water. The hydroxyl radical ($\cdot\text{OH}$) is known to play an important role in the degradation of organic compounds because its oxidation potential can reach 2.8 eV, which is higher than that of other radicals. Further, it can react with most organic substances within a short time; the rate constant of such reactions can reach 10^8 – 10^9 $\text{M}^{-1}\text{s}^{-1}$ [6, 7].

Owing to the high reactivity of $\cdot\text{OH}$ and its short half-life, its direct detection is very difficult to achieve. Therefore, indirect methods have been developed in this regard, one of which is the molecular probe approach [8, 9]. In this study, tert-butanol (TBA) was chosen as the probe given that formaldehyde is formed when it reacts with $\cdot\text{OH}$, which can facilitate its quantification [10, 11]. Furthermore, many long-lived active species, such as O_3 and H_2O_2 , are also considered to be major active species that participate in the degradation of organic contaminants. Therefore, it is very important to analyze the mechanism as well as the rate of formation of these active species that are generated during the NTP discharge process. However, there is a paucity of studies on the generation of active species via various physical and chemical processes that are associated with the discharge process.

Therefore, in this study, the generation of active species during the discharge process was investigated by varying operating parameters, such as initial pH, conductivity, gas flow rate, and liquid circulation rate. Additionally, the various physical and chemical processes that are associated with the discharge process, including UV irradiation, H_2O_2 oxidation, and ozone oxidation, were clarified, and the mechanism of active species generation in both individual and combined oxidation processes was analyzed.

2. EXPERIMENTAL SECTION

2.1. Chemicals and materials

TBA and H_2O_2 were purchased from Aladdin (Shanghai, China), while the other reagents and solvents (analytical grade) used in this study were purchased from Sinopharm Chemical Reagent Co., Ltd. (Beijing, China). All the solutions used in this study were prepared using distilled and deionized water obtained using a Millipore Milli-Q system (Millipore, Massachusetts, USA).

2.2 Experimental setup

The scheme of the NTP reactor, which has been previously described [12, 13], is shown in Figure 1. The reactor was made using glass, and its inner diameter and height were 80 and 100 mm, respectively.

The plasma generator consisted of a hollow gold needle, a concentric dielectric cone-shaped glass tube that enclosed the needle, and a stainless-steel plate beneath them, functioning as the ground electrode. The hollow gold needle doubled as the power electrode and the working gas inlet channel, and the distance between the needle tip and the ground electrode was 10 mm. The discharge generator was powered by a sinusoidal excitation voltage ($V_p = 0\text{--}40$ kV) with a frequency of 0–30 kHz (MeV30KV, Xi'an Zhaofu Electronics Co., Ltd., China). The operating conditions consisted of a discharge power of 50.25 W and an oxygen flow rate of 1.0 L/min. The total volume of the solution in the reactor was 300 mL, and the liquid circulation flow rate was fixed at 150 mL/min, and unless otherwise specified, the test conditions in the experiment remained unchanged.

The pH of the solution, which was adjusted by adding either 0.1 M H_2SO_4 or 0.1 M NaOH , was determined using a portable multi-parameter meter (MultiLine[®] Multi 3620 IDS, Germany). The concentration of H_2O_2 in the solution was measured by the potassium titanium (IV) oxalate method [14], and the concentration of O_3 dissolved in the solution was determined by the indigo method [15]. The gas-phase ozone concentration was monitored using an ozone analyzer (Model 202, 2B Technologies, USA), and the yield of formaldehyde that resulted from the reaction between TBA and $\cdot\text{OH}$ was measured via spectrophotometry (DR5000, HACH, USA). Thus, the yield of $\cdot\text{OH}$, which is twice that of formaldehyde, was calculated according to Equation (1) [10]:

$$k_{\cdot\text{OH}} = \frac{d[\cdot\text{OH}]}{dt} = 2 \frac{d[\text{HCHO}]}{dt}, \quad (1)$$

where $k_{\cdot\text{OH}}$ represents the rate of formation of $\cdot\text{OH}$ ($\text{mg}/(\text{L}\cdot\text{min})$), and $[\cdot\text{OH}]$ and $[\text{HCHO}]$ represent the concentrations of $\cdot\text{OH}$ (mM) and formaldehyde (mg/L) at time t (min), respectively.

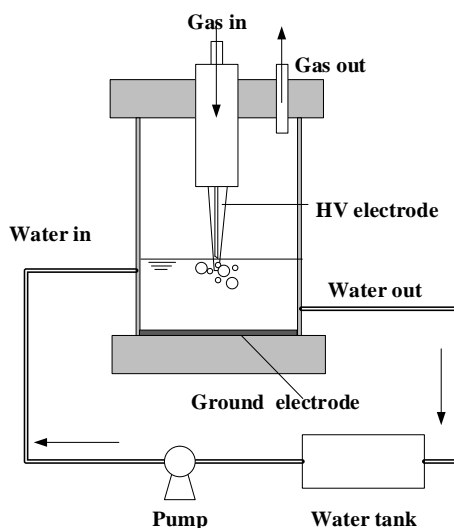


Figure 1. Experimental set-up showing the NTP reactor (Device A).

2.3 Effects of UV irradiation and ozone on the generation of active species

To analyze the effect of UV irradiation on the generation of active species during the oxygen discharge process, the experiments described in the following paragraphs were designed independently.

Based on the original device shown in Figure 1, a circular transparent quartz glass column (5 mm × 5 mm × 50 mm) was placed on tapered quartz glass, as shown in Figure 2. This reactor was referred to as Device B. When oxygen was introduced for the discharge process, UV light was emitted in the quartz glass column (unlike the gas–liquid two-phase discharge power; however, the same intensity of UV irradiation was assumed). The deionized water solution entered the plasma generator through the peristaltic pump, the UV light radiated the solution through the quartz glass tube, and the H₂O₂ output during the reaction was measured.

To reveal the effect of ozone on the generation of active species during the discharge process, the following experiment was conducted. Two discharge devices with identical parameters were designed. The devices were marked Devices A and C, as shown in Figure 3, and as described in Section 2.2, the active exhaust gas produced in Device A was introduced into Device C through a tube, and the resulting active exhaust gas was then introduced into the aqueous solution through the hollow metal tube in Device C. Thereafter, the aqueous solution in Device C was circulated through a peristaltic pump; the influence of the aqueous solution in Device A on ozone could be neglected. Thus, Device C was used to simulate the contribution of ozone only to the generation of active species during discharge.

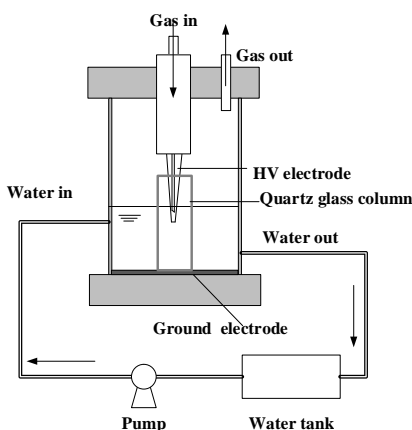


Figure 2. Set-up of UV irradiation only simulator (Device B).

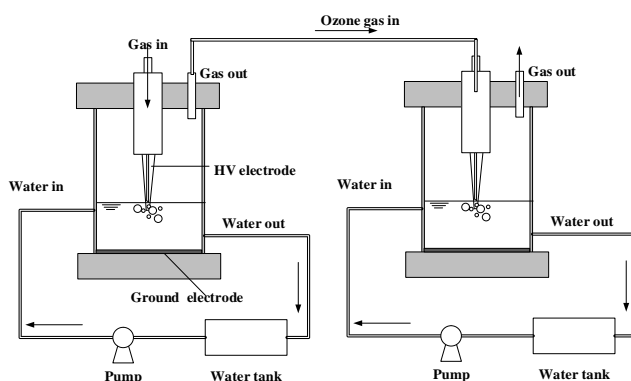


Figure 3. Set-up of ozonation only simulator (left, Device A; right, Device C).

2.4 Effects of the combined processes on the generation of active species

The UV/H₂O₂ simulation test: Under the conditions of experiment 1, a H₂O₂ solution (16 mg/L) was prepared using deionized water, and the change in the concentration of H₂O₂ was investigated under the action of UV radiation during the discharge process. TBA (200 mM) was added to the 16-mg/L H₂O₂ solution, the output of formaldehyde was analyzed, and the output of the combined effect of UV/H₂O₂ on ·OH generation was determined.

The O₃/H₂O₂ simulation test: To analyze the variation of the concentration of H₂O₂ under the action of ozone during the reaction, deionized water was used to prepare a 16-mg/L H₂O₂ solution, which was passed through Device C. TBA (200 mM) was added to the 16-mg/L H₂O₂ solution and the production of formaldehyde was analyzed, and the generation of ·OH owing to the combined effect of O₃/H₂O₂ was quantified.

The UV/O₃ simulation test: Deionized water treatment was performed in Device C for 20 min, and the ozone solution was prepared and passed through device A. The reaction process was analyzed, and the generation of H₂O₂ under UV radiation was determined. TBA (200 mM) was added to the ozone solution and the output of formaldehyde was analyzed, and the output of the combined effect of UV/O₃ on ·OH generation was evaluated.

The UV/O₃/H₂O₂ simulation test: To prepare the ozone solution, deionized water treatment was performed in Device C for 20 min. The deionized water was also used to prepare a 16-mg/L solution of H₂O₂ solution, which was passed through Device A, and the change in the concentration of H₂O₂ owing to the combined action of ozone oxidation and UV irradiation was investigated during the reaction. TBA (200 mM) was added to the 16-mg/L H₂O₂ solution and the production of formaldehyde was analyzed, and the generation ·OH of hydroxyl free radicals owing to UV/O₃/H₂O₂ was quantified.

3. RESULTS AND DISCUSSION

3.1 Effects of different experimental parameters on active species generation

3.1.1 Effect of pH

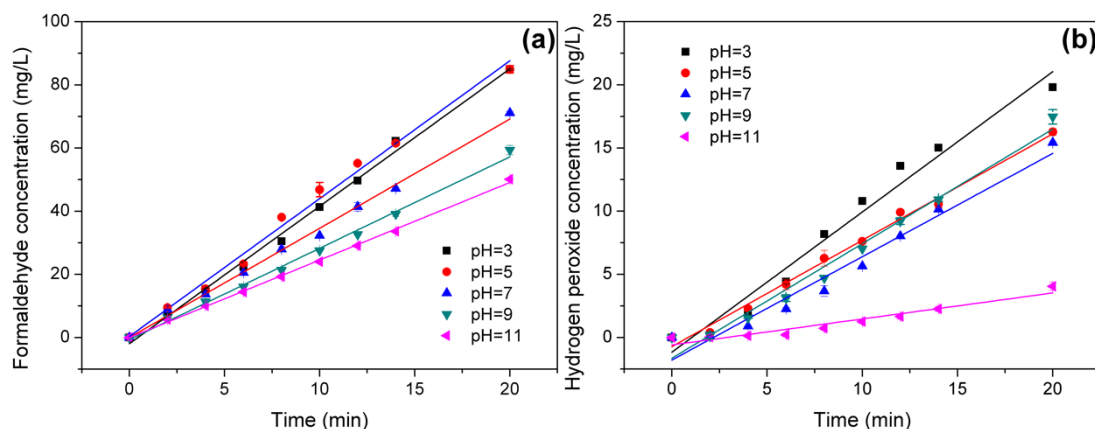
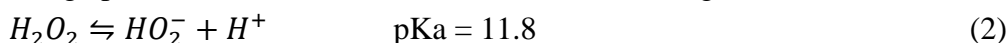
The pH of the solution is an important parameter that influences the reactions occurring in the NTP reactor. This is because pH affects the existence of organic matter in water, the redox potential of active species, and the process of organic matter degradation [16-18]. Under the same discharge conditions, the production of ·OH, H₂O₂, and ozone was investigated during non-thermal discharge at initial pH values of 3, 5, 7, 9, and 11.

As shown in Figure 4, with 200 mM TBA as the ·OH scavenger, the concentration of formaldehyde in the solution increased linearly. After a 20-min discharge process, it was observed that acidic conditions favored ·OH generation. Specifically, when the pH values of the solution were 3 and 5, the concentrations of formaldehyde were 84.8 and 84.9 mg/L, respectively. However, under neutral pH conditions, it was 71.1 mg/L, and under alkaline conditions, specifically at pH values of 9 and 11, it was 59.3 and 50.19 mg/L, respectively. The variation of the concentration of formaldehyde resulting

from the reaction process as a function of pH was fitted into a linear relationship, and an excellent agreement was observed ($R^2 = 0.992\text{--}0.998$). At initial pH values of 3, 5, 7, 9, and 11, the rates of formation of formaldehyde in the solution were 0.145, 0.145, 0.115, 0.096, and 0.082 mM/(L·min), respectively. Using Equation (1), the yield of $\cdot\text{OH}$ was determined to be 0.290, 0.291, 0.237, 0.193, and 0.164 mM/(L·min), respectively.

Similar to formaldehyde, the concentration of H_2O_2 accumulated linearly during the discharge process, and linear fitting yielded R^2 values between 0.975 and 0.992. As shown in Figure 4, under acidic or neutral pH conditions, the H_2O_2 concentration was higher than that observed under alkaline conditions. After discharging for 20 min, when the initial pH of the solution was 3, 5, 7, and 9, there were no significant differences between the observed H_2O_2 concentrations, which were 19.81, 16.27, 15.42, and 17.4 mg/L, respectively. Further, the rates at which H_2O_2 was generated under pH values of 3, 5, 7, and 9 were 1.110, 0.907, 0.842, and 0.818 mg/(L·min), respectively. However, at pH=11, the H_2O_2 concentration was only 4.04 mg/L, and the corresponding generation rate was 0.256 mg/(L·min). This could be mainly attributed to the chemical properties of H_2O_2 ; it is a weak dibasic acid that establishes an ionization equilibrium in solution. Further, when the pH was above 11.8, the ionization balance of H_2O_2 shifted to the right, and decomposition occurred [19].

The solubility of ozone in solution is affected by the pH of the solution [20]. As shown in Figure 4, the concentrations of ozone under acidic and neutral conditions were higher than that observed under alkaline conditions. Specifically, under alkaline conditions, OH^- induced the decomposition of ozone. Further, the concentration of ozone in the liquid phase first increased and then decreased as the reaction progressed, reaching the maximum value at 12–14 min, and then eventually decreasing again. This trend could be primarily attributed to changes in temperature. As the discharge progressed, the temperature of the solution gradually increased. Initially, the temperature of the solution was 25 ± 3 °C. After the 20-min discharge process, it increased to 45 ± 5 °C and this brought a decrease in the solubility of ozone.



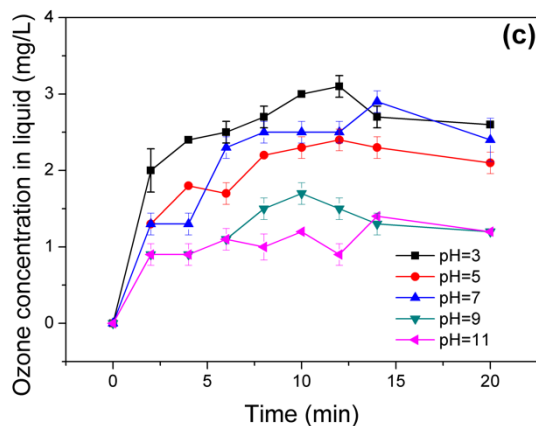


Figure 4. Variation of the concentrations of (a) Formaldehyde, (b) H_2O_2 , and (c) Ozone with time under different pH conditions. (Discharge conditions: 50.25 W discharge power, 1 L/min oxygen flow rate, 150 mL/min liquid flow rate, conductivity was not adjusted)

3.1.2 Effect of conductivity

The effect of conductivity, which was adjusted using a solution of KCl, on H_2O_2 production is shown in Figure 5. From this figure, it is evident that conductivity that values below 50 $\mu\text{S}/\text{cm}$ had no significant impact on H_2O_2 production. Specifically, when the conductivities were 10, 30, and 50 $\mu\text{S}/\text{cm}$, H_2O_2 concentrations obtained after 20 min of discharge were 17.17, 16.24, and 18.91 mg/L, respectively, and the corresponding H_2O_2 generation rates were 0.952, 0.838, and 0.867 mg/L, respectively. However, when the conductivity increased to 100 and 300 $\mu\text{S}/\text{cm}$, there was a drastic drop in the rates of H_2O_2 generation, and at these conductivities, the final H_2O_2 concentrations decreased by 54.24 and 83.73%, respectively, compared with that obtained when the conductivity was 50 $\mu\text{S}/\text{cm}$. Further, at a conductivity of 500 $\mu\text{S}/\text{cm}$, the final concentration of H_2O_2 was 0.587 mg/L. The effect of conductivity on the concentration of the active species was related to the ion composition. When KCl and K_2SO_4 solutions of the same conductivity (500 $\mu\text{S}/\text{cm}$) were used, the concentration of H_2O_2 in the K_2SO_4 solution was significantly higher than that in the KCl solution. When the initial conductivities were 10 and 30 $\mu\text{S}/\text{cm}$, conductivities would increase to above 50 $\mu\text{S}/\text{cm}$ after 2 min of reaction. Furthermore, during the discharge process, the concentration of formaldehyde increased linearly, and after a 20-min discharge, the concentrations of formaldehyde in the solution were 71.10, 62.29, and 51.46 mg/L at conductivities of 10, 30, and 100 $\mu\text{S}/\text{cm}$, and the corresponding formaldehyde formation rates were 3.459, 3.143, and 2.609 mg/(L·min), respectively. The variation of the ozone concentration in the liquid phase was consistent with those of H_2O_2 and formaldehyde. The concentration of ozone in the solution with a lower conductivity was higher than that in the high-conductivity solution; during the discharge process, the concentration of ozone initially increased and then decreased. A possible cause for the observed trend is the increase in the temperature of the solution.

From the above results, it is evident that the yields and rates of the production of active species, namely, $\cdot\text{OH}$, H_2O_2 , and ozone, decrease with increasing conductivity. In a similar study, Shih *et al.* used optical emission spectroscopy to measure the concentration of molecular species (O_3 and H_2O_2)

and free radical species ($\cdot\text{O}$, $\cdot\text{H}$, and $\cdot\text{OH}$), and obtained similar results [3]. As the conductivity of the solution increased, the ion current in the solution increased correspondingly, making the discharge more likely to occur, and the energy released was easily transformed into a thermal effect. Conversely, in the needle-plate discharge reaction device equipped with a hollow needle as the high-voltage electrode, the aqueous solution with a higher conductivity played the role of the ground electrode during the discharge process. The solution was added to the reactor to reduce the distance between the high-voltage electrode and the ground electrode, thereby changing the discharge form, shortening the plasma ion channel, and reducing the number of volume discharge channels [21]. The length of the plasma channel determined the contact area between the plasma and water; this plays an important role in the generation of $\cdot\text{OH}$ as well as other active species, most of which result from the reaction between plasma and water. Therefore, a relatively high solution conductivity hinders the production of active species.

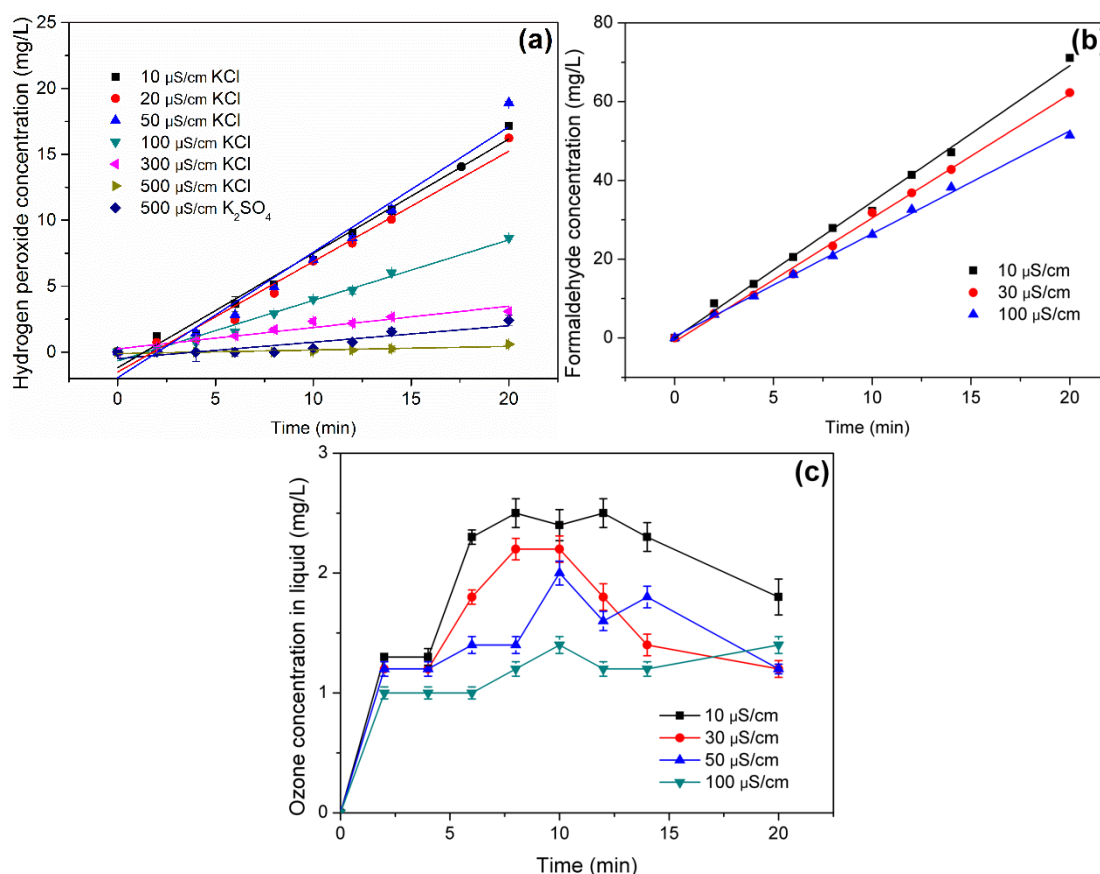


Figure 5. Variation of the concentrations of (a) H_2O_2 (b) $\cdot\text{OH}$, and (c) Ozone with time under different conductivity conditions. (Discharge conditions: 50.25W discharge power, 1 L/min oxygen flow rate, 150 mL/min liquid flow rate, 10 mm electrode gap, pH was not adjusted)

3.1.3 Effect of oxygen flow rate

The effect of the gas flow rate on the generation of active species was analyzed by controlling the oxygen flow rate; the results thus obtained are shown in Figure 6. From this figure, it is evident that at oxygen flow rates of 0.5, 1.0, 1.5, and 2.0 L/min, H_2O_2 concentrations of 17.46, 16.46, 15.42, and 14.27 mg/L, respectively, were obtained after 20 min of discharge, and the corresponding H_2O_2 generation rates were 0.916, 0.862, 0.818, and 0.740 mg/(L·min), respectively. Further, at oxygen flow rates of 0.5, 1.0, 1.5, and 2.0 L/min, the concentrations of formaldehyde were 79.58, 71.11, 77.94, and 82.93 mg/L, respectively, and the corresponding formaldehyde generation rates were 4.395, 3.947, 4.045, and 3.459 mg/(L·min), respectively. The oxygen flow rate had a limited impact on the concentration of ozone in the liquid phase, which however was lower within the first 12 min of gas flow at a rate of 2.0 L/min than at other flow rates. Possibly, this could be attributed to the fact that excessive flow can interrupt the mass transfer of the gas and liquid phases. After 6 min of discharge, the ozone concentration in the gas phase reached an equilibrium state, and at oxygen flow rates of 0.5, 1.0, 1.5, 2.0 L/min, the equilibrium concentrations of ozone in the gas phase were 1497.83, 3661.33, 7360.17 and 9735.53 ppb, respectively.

The gas flow rate had a significant effect on the number of bubbles present in the reactor; thus, it affected the number of burst bubbles as well as the number of active species generated during the reaction. As the gas flow rate increased, the number of bubbles in the reactor increased. Thus, the active species diffused into the liquid phase and reacted with organic matter. For flow rates within a given range, as the gas bubbling flow rate increased, an increasing number of active species were bubbled into the solution to promote the mass transfer of the gas–liquid two-phase reaction. However, further increasing the gas flow rate resulted in a decrease in the residence time and reaction time of the active species. The vigorous gas flow rate caused the small bubbles to merge together into large bubbles, thereby causing the disruption of the gas–liquid mass transfer of the active ingredients. Therefore, when selecting a gas flow rate, it is necessary to consider the balance between the formation of active species and the diffusion and reaction rate characteristics corresponding to the flow rate [5].

Further, as the oxygen flow rate increased, the concentrations of H_2O_2 , OH, and ozone did not change significantly in the liquid environment. However, the concentration of ozone in the gas phase increased significantly upon increasing the gas flow rate. Thus, to improve energy utilization efficiency, it is crucial to understand how to best exploit the ozone generated during the discharge process.

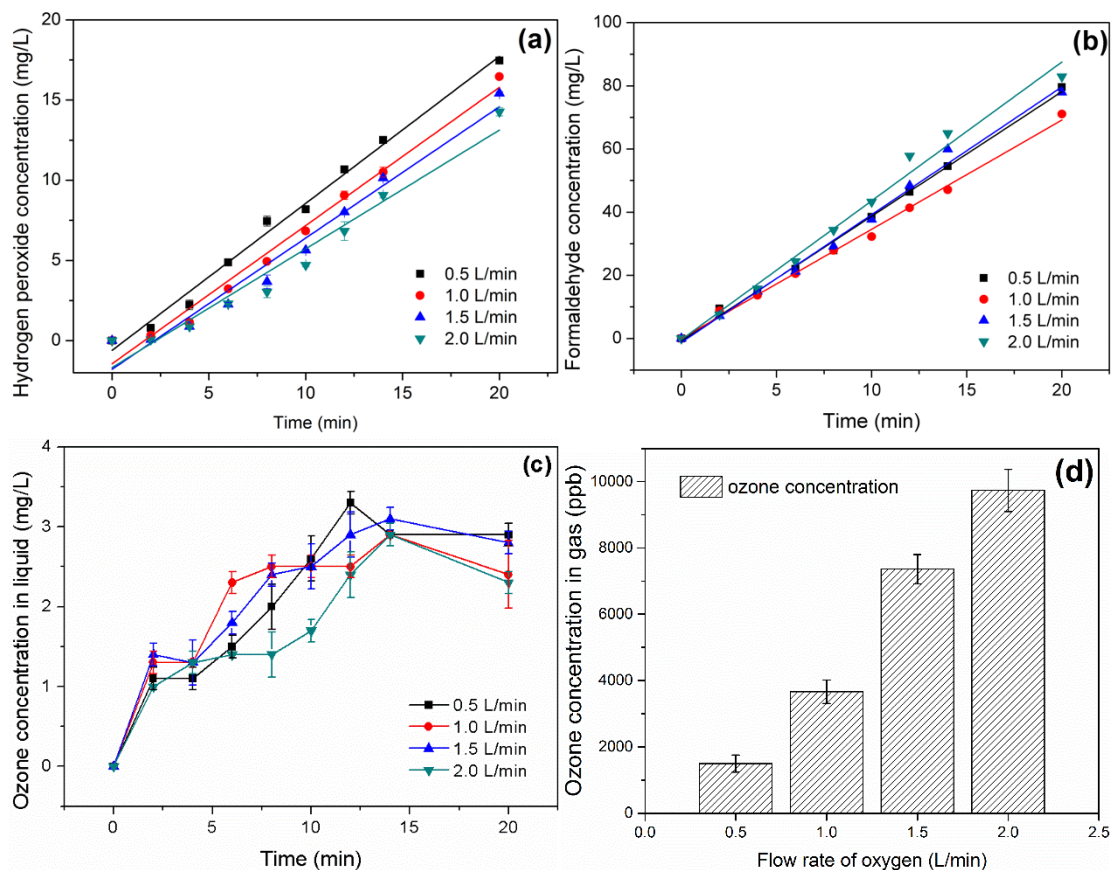


Figure 6. Variation of the concentrations of (a) H₂O₂ (b) Formaldehyde, and (c) Ozone with time at different oxygen flow rates. (d) Variation of ozone concentration with oxygen flow rate. (Discharge conditions: 50.25W discharge power, 150 mL/min liquid flow rate, conductivity and pH were not adjusted).

3.1.4 Effect of solution circulation flow rate

In a plasma water treatment reaction device with internal circulation as the mainstay, the circulation flow rate of the aqueous solution may affect active species generation. Therefore, in this study, the circulation flow rate of the liquid was set to 100, 150, and 200 mL/min using a peristaltic pump, and the residence time of the solution to be treated was set to 3, 2, and 1.5 min, respectively, so as to clarify their effects on active species generation.

As shown in Figure 7, the concentration of H₂O₂ increased linearly during the discharge process, and its accumulation gradually decreased when the solution flow rate was increased. After the 20-min discharge process, and at solution circulation flow rates of 100, 150, and 200 mL/min, H₂O₂ generation rates of 1.0145, 0.5246, and 0.3993 mg/(L·min), respectively, were obtained. Conversely, the solution circulation flow rate had little effect on ·OH generation; the rate of formation of formaldehyde was found to be in the range 4.364–4.006. However, the concentration of ozone in the liquid phase at a circulation flow rate of 200 mL/min was lower than that at other flow rates, possibly because the flow rate was too high, and this had a negative effect on the mass transfer between the gas and liquid phases.

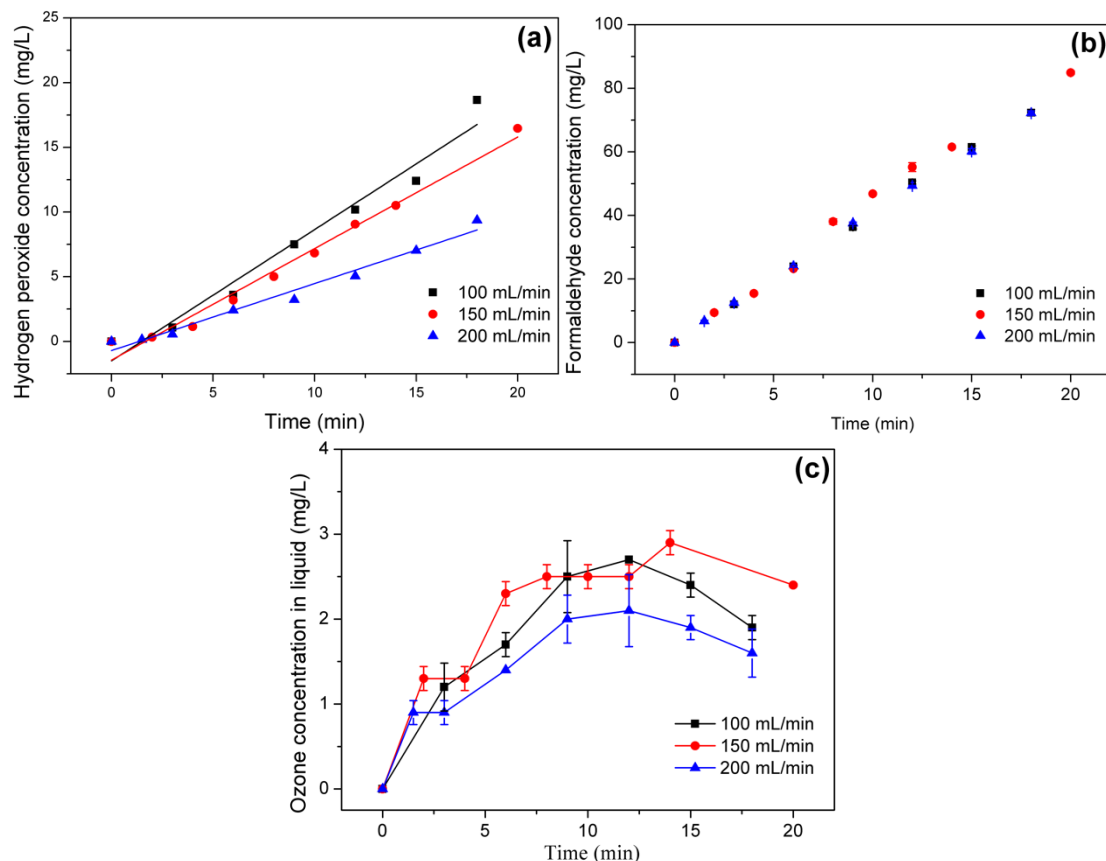


Figure 7. Variation of the concentrations of (a) H_2O_2 (b) Formaldehyde, and (c) Ozone with time at different solution circulation flow rates. (Discharge conditions: 50.25W discharge power, 1 L/min oxygen flow rate, conductivity and pH were not adjusted).

3.2 Effect of different physical and chemical processes on active species generation

The gas–liquid NTP-based degradation of organic matter involves a variety of physical and chemical processes, including UV irradiation, H_2O_2 oxidation, and ozone oxidation, and an important research focus in this regard is to reveal the source of $\cdot\text{OH}$ as well as the effect of various physical and chemical processes on the generation of active species. By simply decomposing and removing uncertain processes, such as the movement of shock waves, when oxygen is used as the discharge gas source, the NTP process can be decomposed into individual oxidation technologies as well as combined technologies. The individual technologies include UV irradiation, H_2O_2 oxidation, and O_3 oxidation, whereas the combined processes include $\text{UV}+\text{H}_2\text{O}_2$, $\text{O}_3+\text{H}_2\text{O}_2$, $\text{UV}+\text{O}_3+\text{H}_2\text{O}_2$, and $\text{UV}+\text{O}_3$.

3.2.1 Effect of individual oxidation processes

During the water treatment process, UV radiation is often used for disinfection; however, in advanced oxidation technologies, it can directly or indirectly bring about the degradation of organic matter [22, 23]. The conversion of electrical energy to light energy is realized during the discharge

process owing to the associated electron energy level transition, which makes the occurrence of photochemical processes in the plasma reaction device possible [24, 25]. The absorption of UV light led to the direct photolysis of photolabile compounds or indirect photolysis involving H_2O_2 to generate $\cdot\text{OH}$, which degrades organic compounds.

As shown in Figure 8, under UV light irradiation, basically no H_2O_2 was detected after 20 min of reaction. This observation may be attributed to the fact that the proportion of light emitted by the plasma with a wavelength below 254 nm is relatively small and has low energy; thus, preventing the possibility of achieving effective radiation. To analyze the impact of UV irradiation on the generation of active species, a quartz tube sleeve was placed outside the high-voltage end of the plasma-needle plate so as to extend the distance traveled by the UV irradiation to a certain extent, thereby increasing the energy attenuation caused by propagation. The results obtained show that UV radiation has little effect on the production of active species in the needle-plate gas-liquid two-phase discharge device used in this experiment.

Similar results were obtained following an analysis of the influence of ozone oxidation only on the generation of active species, as almost no H_2O_2 was detected under the action of UV or ozone. Additionally, no reaction was observed between water and ozone; however, under alkaline conditions (pH = 10), a small amount of H_2O_2 , with a concentration below 5 mg/L, was detected. This is because alkaline environments induce the decomposition of ozone as well as the production of $\cdot\text{OH}$, which undergoes a chain reaction to produce a small amount of H_2O_2 . The above results show that, in this NTP device, individually, both UV radiation and ozone oxidation have little effect on the production of active species.

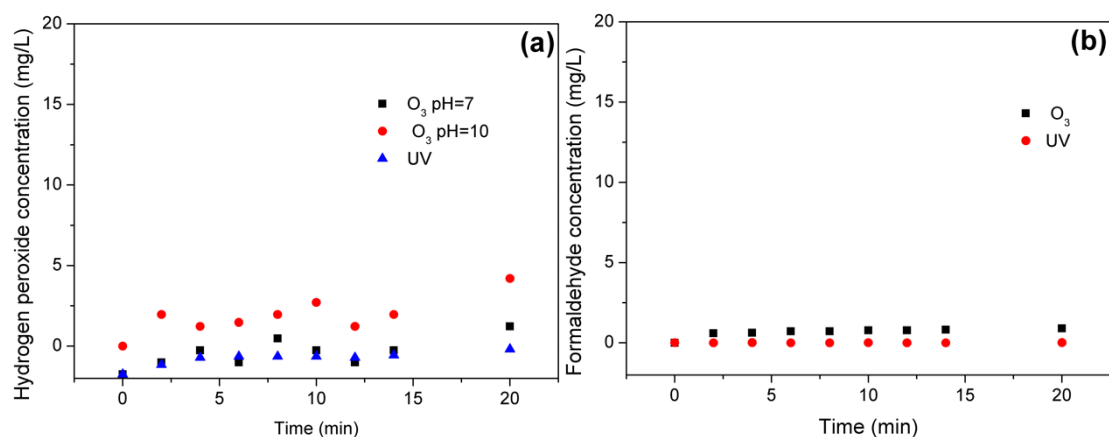


Figure 8. Influence of ozone oxidation and UV radiation on the concentration of (a) H_2O_2 and (b) Formaldehyde. (Discharge conditions: 50.25W discharge power, 1 L/min oxygen flow rate, 150 mL/min liquid flow rate, conductivity and pH was not adjusted).

3.2.2 Effect of combined processes

During the non-thermal discharge process, UV radiation, O_3 oxidation, and H_2O_2 oxidation can induce a variety of oxidation processes[26]. Four different sets of experiments involving various

combinations of UV radiation, O₃ oxidation, and H₂O₂ oxidation were performed to analyze the production of ·OH and to reveal the decomposition of H₂O₂ by UV radiation, ozone oxidation, and H₂O₂ oxidation or various combinations of these processes (i.e., UV/H₂O₂, O₃/H₂O₂, UV/O₃/H₂O₂, and UV/O₃) during the active species generation process. In the experiments presented in Section 2.3, the maximum accumulation of H₂O₂ after 20 min of discharge was 16 mg/L. The initial concentration of H₂O₂ in the control solution was set to 16 mg/L so as to simulate the participation of H₂O₂ in the formation of active species during the discharge process.

During its generation process, H₂O₂ was decomposed by UV light, ozone, and the combined action of the two processes[27, 28]. To reveal the influence of these physical and chemical processes on the decomposition of H₂O₂ during the discharge process, a 16 mg/L H₂O₂ solution was passed through the UV irradiation emitted by the plasma device; thus, the concentration of H₂O₂ decreased gradually. Further, under the action of UV light and ozone, H₂O₂ decomposed, and its concentration decreased by 28.3 and 65.2%, respectively. This implies that ozone showed a greater tendency to promote the decomposition of H₂O₂. When ozone and UV light worked together, basically no H₂O₂ was detected after 10 min of reaction. Under the same conditions, the concentration of formaldehyde increased linearly following the addition of TBA (200 mM) under UV irradiation. After 20 min of reaction, the concentration of formaldehyde was 9.19 mg/L and the corresponding generation rate was 0.3992 mg/(L·min).

As shown in Figure 9, in the UV/O₃/H₂O₂ and UV/O₃ sets of experiments, the concentrations of formaldehyde increased linearly, and were 75.55 and 72.52 mg/L, respectively after 20 min of reaction. Additionally, the corresponding formaldehyde generation rates were 3.836 and 3.690 mg/(L·min), respectively. The experiments involving O₃/H₂O₂ and UV/H₂O₂ resulted in formaldehyde concentrations of 9.19 and 19.14 mg/L, respectively, after 20 min of reaction. In the O₃/H₂O₂ experiment, the concentration of formaldehyde gradually increased within the first 12 min and then remained constant. After 20 min of reaction, the rate of formaldehyde generation was 0.883 mg/(L·min), and its concentration remained unchanged after 12 min. In the UV/H₂O₂ experiment, the concentration of formaldehyde increased slowly, reaching only 0.399 mg/(L·min). Further, in the analysis of the decomposition of H₂O₂ induced by UV irradiation and O₃ oxidation, the ratios of the decomposition rate constants of H₂O₂ to the generation rates of formaldehyde were 0.64 and 0.596, respectively. The difference in the ratios corresponding to these two sets of experiments was not significant. Therefore, it is plausible to infer that the generation of ·OH in the O₃/H₂O₂ and UV/H₂O₂ experiments originated from H₂O₂ decomposition. The promoting effect of H₂O₂ on the generation of hydroxyl radicals has also been observed in previous studies[27, 29, 30]. The results of these experiments demonstrate that individually, ozone and UV light do not contribute significantly to the production of formaldehyde under the test conditions.

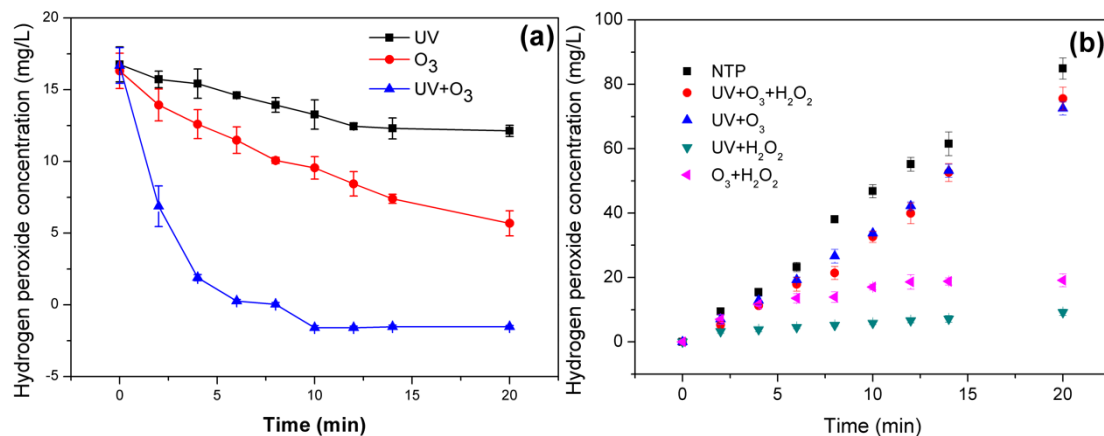


Figure 9. Variation of the concentration of H₂O₂ under (a) Individual processes and (b) Combined processes. (Discharge conditions: 50.25W discharge power, 1 L/min oxygen flow rate, 150 mL/min liquid flow rate, conductivity and pH were not adjusted)

4. CONCLUSIONS

In this study, a needle-plate gas–liquid phase NTP discharge device with oxygen flow was used to quantitatively determine the production of active species, namely, $\cdot\text{OH}$, H₂O₂, and O₃, and TBA was chosen as a scavenger of $\cdot\text{OH}$ given that it reacts with $\cdot\text{OH}$ to form formaldehyde, a specific product that can be used to quantify the generation of $\cdot\text{OH}$. The influence of several factors on the generation of these active species was investigated during the discharge process, and it was observed that the yields of $\cdot\text{OH}$ and H₂O₂ were the highest under acidic conditions, but medium and the lowest under neutral and alkaline conditions, respectively. It was also observed that solutions with high-conductivity did not favor the production of active species, and the yield of the active species was also found to be related to the electrolyte type. Further, it was observed that the oxygen and liquid circulation flow rates have little effect on the generation of $\cdot\text{OH}$ and H₂O₂ in aqueous solutions; however, they showed a greater impact on the mass transfer of ozone in the gas and liquid phases. Furthermore, the results of simulation experiments demonstrated that individually, UV radiation and ozone oxidation processes have little effect on active species generation. However, the combination of multiple processes could significantly promote the production of active species.

ACKNOWLEDGEMENT

This work was supported by the National Natural Science Foundation of China (grant number 51578309).

References

1. J. Shen, H. Zhang, Z. Xu, Z. Zhang, C. Cheng, G. Ni, Y. Lan, Y. Meng, W. Xia, P.K. Chu, *Chem. Eng. J.*, 362 (2019) 402.
2. B. Jiang, J. Zheng, S. Qiu, M. Wu, Q. Zhang, Z. Yan, Q. Xue, *Chem. Eng. J.*, 236 (2014) 348.
3. H. Xu, R. Ma, Y. Zhu, M. Du, H. Zhang, Z. Jiao, *Sci. Total Environ.*, 703 (2020) 134965.

4. S. Tang, N. Li, J. Qi, D. Yuan, J. Li, *Plasma Sci. Technol.*, 20 (2018) 054013.
5. Q. Zhang, H. Zhang, Q. Zhang, Q. Huang, *Chemosphere*, 210 (2018) 433.
6. C. Zhang, L. Gu, Y. Lin, Y. Wang, D. Fu, Z. Gu, *J. Photochem. Photobiol., A*, 207 (2009) 66.
7. T. Wang, G. Qu, J. Ren, Q. Yan, Q. Sun, D. Liang, S. Hu, *Water Res.*, 89 (2016) 28.
8. S. Tang, D. Yuan, Y. Rao, J. Zhang, Y. Qu, J. Gu, *J. Environ. Manage.*, 226 (2018) 22.
9. K.C. Hsieh, R.J. Wandell, S. Bresch, B.R. Locke, *Plasma Processes Polym.*, 14 (2017).
10. H. Wang, J. Zhan, W. Yao, B. Wang, S. Deng, J. Huang, G. Yu, Y. Wang, *Water Res.*, 130 (2017) 127.
11. A. Tekle-Röttering, E. Reisz, K.S. Jewell, H.V. Lutze, T.A. Ternes, W. Schmidt, T.C. Schmidt, *Water Res.*, 102 (2016) 582.
12. Y. Xin, L. Zhou, K. Ma, J. Lee, H.I.A. Qazi, H. Li, C. Bao, Y. Zhou, *J. Water Process Eng.*, 37 (2020) 101457.
13. K. Ma, Z. Ren, L. Zhou, Y. Bai, Y. Xin, H. Li, C. Bao, Y. Zhou, *In. J. Electrochem. Sci.*, (2021) 210345.
14. P. Vanraes, G. Willems, N. Daels, S.W.H. Van Hulle, K. De Clerck, P. Surmont, F. Lynen, J. Vandamme, J. Van Durme, A. Nikiforov, C. Leys, *Water Res.*, 72 (2015) 361.
15. H. Bader, J. Hoigné, *Water Res.*, 15 (1981) 449.
16. F. Huang, L. Chen, H. Wang, Z. Yan, *Chem. Eng. J.*, 162 (2010) 250.
17. J. Ding, L. Shen, R. Yan, S. Lu, Y. Zhang, X. Zhang, H. Zhang, *Chemosphere*, 261 (2020) 127715.
18. M.G. Antoniou, A.A. de la Cruz, D.D. Dionysiou, *Appl. Catal., B*, 96 (2010) 290.
19. B.R. Locke, S.M. Thagard, *Plasma Chem. Plasma Process.*, 32 (2012) 875.
20. K.M.S. Hansen, A. Spiliotopoulou, R.K. Chhetri, M. Escolà Casas, K. Bester, H.R. Andersen, *Chem. Eng. J.*, 290 (2016) 507.
21. H. Wang, R.J. Wandell, K. Tachibana, J. Voráč, B.R. Locke, *J. Phys. D: Appl. Phys.*, 52 (2019).
22. L. Varanasi, E. Coscarelli, M. Khaksari, L.R. Mazzoleni, D. Minakata, *Water Res.*, 135 (2018) 22.
23. H.R. Sindelar, M.T. Brown, T.H. Boyer, *Chemosphere*, 105 (2014) 112.
24. H. Lee, Y.K. Park, J.S. Kim, Y.H. Park, S.C. Jung, *Environ. Res.*, 169 (2019) 256.
25. H. Guo, N. Jiang, H. Wang, K. Shang, N. Lu, J. Li, Y. Wu, *Appl. Catal., B*, 248 (2019) 552
26. H. Zeghioud, P. Nguyen-Tri, L. Khezami, A. Amrane, A.A. Assadi, *J. Water Process Eng.*, 38 (2020) 101664.
27. G. Iervolino, V. Vaiano, V. Palma, *Environ. Technol. Innovation*, 19 (2020) 100969.
28. R.P. Joshi, S.M. Thagard, *Plasma Chem. Plasma Process.*, 33 (2013) 17.
29. M.C. Collivignarelli, R. Pedrazzani, S. Sorlini, A. Abbà, G. Bertanza, *Sustainability*, 9 (2017) 244.
30. G. Son, D.-h. Kim, J.S. Lee, H. Lee, *Chemosphere*, 157 (2016) 271.